Genomic signatures of introgression at late stages of speciation in a malaria mosquito

Colince Kamdem[1]*, Caroline Fouet[1], Stephanie Gamez[1], Bradley J. White[1,2]*

[1]Department of Entomology, University of California, Riverside, CA 92521

[2]Center for Disease Vector Research, Institute for Integrative Genome Biology, University of California, Riverside, CA 92521

*Corresponding authors: colincek@ucr.edu; bwhite@ucr.edu

Key words: Introgression, speciation, linkage disequilibrium, divergent selection, *Anopheles nili*

Abstract

Hybridization plays a central role during the evolution of species boundaries, but the relative impact of gene flow on genomic divergence and vice versa remains largely unknown. The genome architecture of populations and emerging species exhibiting various levels of divergence along the speciation continuum should provide insights into the events that promote or prevent speciation. In this work, we have used a combination of population genomic approaches to examine the genomic signatures of hybridization between *Anopheles nili sensu stricto* and *An. ovengensis*, two malaria mosquitoes that have split ~3-Myr ago. Despite this substantial time since divergence, the two species hybridize extensively in nature, giving rise to a unique population of differentiated hybrids in contact zones. Using genomic clines and Bayesian models, we showed that signatures of introgression are widespread across the genome suggesting that recent hybridization between *Anopheles nili sensu stricto* and *An. ovengensis* involves multiple fitness traits and functional classes. Linkage Disequilibrium analyses allowed us to identified a block of 39 linked loci that segregated between hybrids and parental species and may harbour genes responsible for reproductive isolation. Our results demonstrate that genome-wide admixtures can persist in the face of species divergence over long periods of time during speciation due to increased gene flow at loci providing selective advantage.

Introduction

Most cases of speciation occur in a gradual manner so that emerging species continue to mate and exchange genes before the onset of complete reproductive isolation (Nosil 2012; Nadeau *et al.* 2013). As a result, secondary contacts between diverging lineages are pervasive in nature and can lead to several scenarios including extensive hybridization and the creation of a new hybrid species or genetic homogenization (James 2007; Ozerov *et al.* 2016). The role of hybridization either in the creation of biodiversity through speciation or in its reduction through genetic homogenization has been under increasing scrutiny over the last decades and has been recognized as one major force driving the evolution of plant and animal species (James 2007; Abbott *et al.* 2013; Mallet *et al.* 2015). However, although there is consistent evidence that hybridization can provide the raw material for evolutionary diversification (Grant 2015), examples of homoploid hybrid species (where the hybrid offspring has the same ploidy level as the two parental species) are rather rare in nature (James 2007; Abbott *et al.* 2013). Most often, hybrids have reduced fitness relative to parental populations and barely persist as a reproductively isolated unit in the wild.

It is particularly difficult to predict the outcome of secondary contacts between diverging lineages and specifically the rate of hybridization (Payseur & Rieseberg 2016). One main issue is that the level of divergence between species supposed to encourage or prevent hybridization remains obscure. Until a recent past, estimates of the population differentiation parameter F_{ST} have been used to predict the rate of hybridization between incomplete species. Variations in F_{ST} among groups of related species were often

interpreted as indicative of differences in rates of gene flow across populations, high F_{ST} values being considered as evidence of limited gene flow. However, instances of hybridization and introgression between highly divergent taxa are accumulating, thereby indicating that estimates of population differentiation are particularly poor predictors of hybridization between two species (Nydam & Harrison 2011; Roux *et al.* 2013; Parchman *et al.* 2013; Martin *et al.* 2013; Canestrelli *et al.* 2014).

Likewise, genomic regions showing high differentiation among populations have been thought to harbor hybrid incompatibility or other reproductive isolation (RI) factors. In support of this view, genome scans in many couples of incipient species have identified genomic regions of extreme F_{ST} values qualified as "speciation islands", considered to be enriched in RI factors and resistant to gene flow (Turner *et al.* 2005; Hohenlohe *et al.* 2010; Lawniczak *et al.* 2010; Ellegren *et al.* 2012). Yet, not only cases where genes involved in RI have been explicitly identified in F_{ST} outliers regions of the genome are extremely rare, but also extensive introgression has been found to sometimes coincide with regions of high differentiation. For example, (Parchman *et al.* 2013) used genomic clines and Bayesian models to study the correlation between regions of exceptional introgression and genetic differentiation manakins birds (*Manacus*). Contrary to expectations, they found that loci of strong introgression were relatively positively correlated to the genetic differentiation. The most plausible interpretation of this intriguing result is that divergent selection may promote introgression of select genes or genomic regions, resulting in differential patterns of introgression across the genome. A relative concordance between locus-specific

74 divergence and locus-specific measures of introgression has also been described in the
75 *Lycaeides* butterfly (Gompert *et al.* 2012, 2013) and in *Drosophila melanogaster* (Pool *et al.*
76 2012). Overall, the relationship between introgressive hybridization and genetic divergence
77 at the species or the genome level is more complex than previously thought. Whether
78 exceptionally differentiated regions of the genome harbor genes that can, paradoxically,
79 introgress easily is an empirical question that remains opened and should be answered by
80 studying closely related species at hybrid zones.
81
82 Mosquitoes of the genus *Anopheles* are ideal system in which to address the evolutionary
83 processes at hybrid zones due to the prevalence of adaptive speciation (Ndo *et al.* 2013;
84 Neafsey *et al.* 2015; Kamdem *et al.* 2016). In this paper, we focused on *An. nili*, a group of
85 African malaria vectors characterized by a reticulate evolution leading to complex
86 phylogenies that have been challenging to clarify (Kengne *et al.* 2003; Awono-Ambene *et al.*
87 2004, 2006; Ndo *et al.* 2010, 2013; Peery *et al.* 2011; Sharakhova *et al.* 2013). The group
88 harbour four known species identified by slight morphological differences: *An. nili sensu*
89 *stricto*, *An. ovengensis*, *An. carnevalei*, and *An. somalicus*. *An. nili sensu stricto* (thereafter *An.*
90 *nili*) is the most widespread across the continent while the three other species are more
91 patchily distributed primarily in the equatorial rainforest. *An. nili* and *An. ovengensis* are
92 important vectors of human malaria parasites (Antonio-Nkondjio *et al.* 2006). We sampled
93 populations across the ranges of the four species of the *An. nili* group in Cameroon and we
94 used a population resequencing approach to develop genome-wide SNP markers that we
95 genotyped in 145 individuals. Our first aim was to clarify the evolutionary relationships

96 between populations. We discovered new cryptic species within *An. ovengensis* and *An. nili*
97 as well as a hybrid subgroup resulting from massive hybridization in sympatric areas.
98 Finally, we took advantage of the recent implementation of genomic cline models that
99 enables the investigation of footprints of introgression across genomes of non-model
100 organisms without the need of a high-quality reference genome (Gompert & Alex 2011;
101 Gompert & Buerkle 2012), to critically evaluate the interplays between the locus-specific
102 divergent selection and introgression.

Materials and methods

Mosquito sample

We surveyed a total of 28 geographic locations that were representative of the main habitats of species of the *An. nili* group previously described in Cameroon (Fig 1A) (Awono-Ambene *et al.* 2004, 2006; Antonio-Nkondjio *et al.* 2009; Ndo *et al.* 2010, 2013). The different species were identified using reference morphological identification keys and a diagnostic PCR that discriminates the four currently known members of the *An. nili.* group on the basis of a point mutation of the ribosomal DNA (Gillies & De Meillon 1968; Gillies & Coetzee 1987; Kengne *et al.* 2003).

Library preparation, sequencing and SNP discovery

We created double-digest RAD (ddRAD) libraries using a modified version of the protocol described by Peterson et al, 2012 (Peterson *et al.* 2012). Genomic DNA of mosquitoes was extracted using the DNeasy Blood and Tissue kit (Qiagen) and the Zymo Research MinPrep kit on larvae and adult samples respectively. Approximately 50 ng (10µl) of DNA of each mosquito sample was digested simultaneously with *MluC1* and *NlaIII* restriction enzymes. Digested products were then ligated to adapter and barcode sequences to enable the unique identification of the individual associated with each sequencing read. The samples were pooled, purified, and 400-bp fragments selected. The resulting libraries were then amplified via PCR and purified. The distribution of library fragment-size was checked on a BioAnalyzer (Agilent Technologies, Inc., USA). The PCR products were quantified and diluted for sequencing on Illumina HiSeq2000 (Illumina Inc., USA) to yield single-end reads of 101 bp.

125 **Bioinformatics pipeline**

126 The *An. nili* Dinderesso draft genome assembly comprises 51,048 contigs, varying between
127 100 and 26775kb in length, to which short reads can be aligned and SNP called. However,
128 members of the *An. nili* group found in Cameroon diverged ~0.2-6 million years ago (Ndo *et*
129 *al.* 2013). Thus, alignments of our samples to *An. nili* Dinderesso reference genome might be
130 subjected to an important bias associated with the inconsistent mapping of reads from
131 highly divergent populations. To make sure that this potential reference sequence bias
132 didn't undermined our analyses, we compared our results across two SNP sets that were
133 identified within RAD loci created using two distinct approaches: a *de novo* assembly and an
134 assembly of reads aligned onto the reference genome. Recent studies using RAD sequencing
135 on *Heliconius* butterflies showed that combining *de novo* assemblies and reference
136 alignments provided a robust approach to perform rigorous test on introgression and
137 phylogenetic relationships in distantly related species (The Heliconius Genome Consortium
138 2012). The *process_radtags* program of the Stacks v 1.35 pipeline was used to demultiplex
139 and clean raw reads. Reads without the *NlaIII* restriction site and those bearing ambiguous
140 barcode sequences or having low-quality score (average Phred score < 33) were discarded.
141 Reads were trimmed to 96-bp by removing index and barcode sequences. We aligned the
142 short reads to the *An. nili* Dinderesso draft genome assembly using Gsnap (Wu & Nacu
143 2010) with a maximum of five nucleotide mismatches allowed. The *ref_map.pl* and
144 *denovo_map.pl* programs in Stacks were used to identify consensus RAD loci and to call
145 SNPs within these loci across our populations using respectively the Gsnap-aligned SAM
146 files or the individual fastq files as input. For both analyses, we set the minimum number of

147 reads required to form a stack to 3. In the *denovo* assembly, we allowed a maximum of three
148 mismatches when creating loci in every individual (M parameter in *denovo_map.pl*) and two
149 mismatches when building the catalogue of loci across individuals (n parameter). In
150 reference-based assembly, we specified n = 2 in *ref_map.pl* to allow two mismatches during
151 catalogue creation. We generated SNP files in different formats for further downstream
152 analyses using the *populations* program of Stacks and PLINK v1.09 (Purcell *et al.* 2007).

153 **Population genetic structure**

154 We analyzed the genetic structure of *An. nili s.l.* populations using Principal Component
155 Analysis (PCA) and Neighbor-Joining trees (NJ). We also examined ancestry proportions
156 and admixtures between populations in ADMIXTURE v1.23 (Alexander *et al.* 2009) and
157 STRUCTURE v2.3.4 (Pritchard *et al.* 2000). We performed these tests using filtered SNPs
158 identified in RAD loci present in every population and in at least 50% of individuals by the
159 *populations* program in Stacks. We used the R package *adegenet* (Jombart 2008) to
160 implement the PCA. Neighbor-Joining trees were generated from matrixes of Euclidian
161 distance computed from allele frequencies at genome-wide SNPs using the R package *ape*
162 (Paradis *et al.* 2004). We ran ADMIXTURE with 10-fold cross-validation for values of k from
163 1 through 20. We analyzed patterns of ancestry from k ancestral populations in
164 STRUCTURE, testing five replicates of k = 1-10. We used 200000 iterations and discarded
165 the first 50000 iterations as burn-in for each STRUCTURE run. CLUMPP v1.1.2 (Jakobsson &
166 Rosenberg 2007) was used to summarize assignment results across independent runs and
167 DISTRUCT v1.1 (Rosenberg 2004) to plot STRUCTURE results. To identify the optimal
168 number of genetic clusters in our samples, we used simultaneously the lowest cross-

validation error in ADMIXTURE, the ad-hoc statistic deltaK (Evanno *et al.* 2005; Earl & VonHoldt 2012) and the Discriminant Analysis of Principal Component (DAPC) method in *adegenet*.

Population genomics analyses

To quantify the genetic differentiation between species and putative subgroups within species, we used a subset of 1000 high-quality SNPs to calculate the overall pairwise differentiation index F_{ST} (Weir & Cockerham 1984) in Genodive v 1.06 (Meirmans & Van Tienderen 2004). Statistical significance was assessed with 10000 permutations. To further examine the genomic footprints of selection and introgression, we used ANGSD v 0.612 (Korneliussen *et al.* 2014) and ngsTools (Fumagalli *et al.* 2014) to derive locus-specific estimates of the nucleotide diversity (measured as θ_w and θ_π), Tajima's *D*, absolute sequence divergence (d_{xy}) and F_{ST} across 9622 sites using Gnap alignments without SNP calling. To identify statistical outliers of F_{ST}, we used the software LOSITAN which applies the coalescent simulation method (FDIST2) (Beaumont & Nichols 1996) to identify loci with exceptionally high F_{ST} values relative to a "neutral" genome-wide F_{ST} value expected under neutral evolution. We ran LOSITAN using the neutral F_{ST} option, 50,000 simulations and a false discovery rate of 0.05%. Finally, we used the R package LDna (Kemppainen *et al.* 2015) for identifying clusters of linkage disequilibrium in our samples. This analysis was conducted primarily to assess the possible influence of inversion polymorphism on the genomic architecture of divergence and hybridization. Precisely, we wished to test if loci with great significance in the genetic divergence and/or introgression were independent loci scattered throughout the genome or clusters of linked loci encapsulated in low

recombination regions like chromosomal inversions. We used PLINK to calculate the linkage disequilibrium (estimated as the r^2 correlation coefficient) between all pairs of SNPs and we applied the graph-based method implemented in LDna to search for clusters of strongly correlated SNPs.

Tests of introgression

In addition to the interpretation of patterns of ancestry provided by clustering analyses in STRUCTURE and ADMIXTURE, we conducted formal tests to infer the history of population splits and admixtures. We used the three-population (f_3) and the four-population (f_4) statistics, introduced in (Reich *et al.* 2009) as methods to estimate mixture proportions in an admixed group, to test for introgression among species. The f_3 and f_4 statistics exploit the idea that the genetic drift, defined as a function of allele frequency, should be uncorrelated in unadmixed populations. As a result, correlations detected between allele frequencies of three (f_3) or four (f_4) populations joined by an unrooted tree indicate episodes of gene flow. Specifically, the f_3 (X; Y, W) tests for admixture between a test population X and two reference populations Y and W. The expected value of f_3 is positive in case of no mixture and negative if X is admixed with Y or W, or both. Similarly, the f_4 for an unrooted tree (A,B;C,D), tests whether allele frequency differences between A and B are correlated with differences between C and D. f_4 is equal to zero if there are no correlations and no admixtures across branches of the tree. In contrast, f_4 is significantly positive if admixture occurs between A and C, or between B and D, or both, and significantly negative if admixture occurs between A and D, or between B and C, or both. The statistical significance of f_3 and f_4 values is assessed using a Z-score: an f_3 or f_4 value divided by its standard deviation. We used a

213 threshold Z-score of 2.5 corresponding to a p-value of 0.05 as suggested in (Reich *et al.*
214 2009). The *threepop* and *fourpop* programs of the software *TreeMix* (Pickrell & Pritchard
215 2012) were used to calculate f_3 and f_4 statistics and Z-scores for all possible triples and
216 quadruples of populations we described within *An. nili s.l.*
217 We next applied the graph-based method developed in *TreeMix* to determine the
218 directionality and quantify the extent of gene flow among species. The *TreeMix* approach
219 uses allele frequencies at genome-wide polymorphisms and a Gaussian approximation of
220 the genetic drift among populations to first construct a Maximum Likelihood (ML)
221 phylogeny connecting sampled populations by simple bifurcations. The model then
222 compares the covariance structure modeled by this dendrogram and adds edges to the
223 phylogeny to account for admixtures. We first conducted one *TreeMix* run without
224 migration. We noted the percentage of explained variance of the models and visually
225 inspected the residuals of covariance matrixes among populations. We next ran *TreeMix*
226 100 times without migration using different numbers of random seed and we built a ML
227 consensus tree from the 100 trees in *SumTrees* (Sukumaran & Holder 2010) using the 95%
228 majority rule. We finally added 1 and 4 migration edges to the ML trees and examined the
229 changes in the percentage of explained variance and the residual fit. For all f_3, f_4 and
230 *TreeMix* analyses, we used 4343 SNPs that were present in all populations and in at least
231 50% of individuals in every population.
232 **Genomic clines**
233 Loci of exceptional introgression compared with genome-wide average admixture may be
234 important for local adaptation or the maintenance of species barriers. To identify sites with

235 the greatest contribution to introgression between *An. nili* and *An. ovengensis*, we used the
236 Bayesian model of genomic clines as implemented in *bgc* (Gompert & Buerkle 2012). The
237 model first estimates a genome-wide average of a hybrid index (*h*) that varies between zero
238 and one for every potentially admixed individual, using allele frequencies of "pure" parental
239 populations (Gompert & Alex 2011). The value zero corresponds to pure individuals of the
240 alternative species (*An. ovengensis* in our case) and the value one to pure individuals of the
241 reference species (*An. nili* in our case). Two genomic clines parameters α and β are then
242 used to evaluate the deviation of individual loci in admixed individuals from the expected
243 genome-wide hybrid index (*h*). The cline parameter α reflects the probability of *An. nili*
244 ancestry relative to the base expectation (*h*), whereas the genomic cline parameter β
245 denotes the rate of transition from low to high probability of *An. ovengensis* ancestry as a
246 function of hybrid index (Gompert & Alex 2011). Deviations of loci from the genome-wide
247 average of α and β were examined on the basis of departures from the 95% confidence
248 envelope.
249 The "pure" parental populations we used in genomic clines analyses were apparently
250 allopatric *An. nili* and *An. ovengensis* populations collected in Nyabessan and Nkoteng,
251 respectively (Fig. 1A). The two locations are separated by ~420 km, which presumably
252 reduces the rate of gene flow between *An. nili* and *An. ovengensis*. Hybrids were admixed
253 individuals collected from the sympatric area in Mbébé (Fig. 1A). These individuals had
254 almost equivalent ancestry proportions from *An. nili* and *An. ovengensis* as revealed by both
255 STRUCTURE and ADMIXTURE clustering analyses. In *bgc*, we estimated genomic cline
256 parameters using 9622 SNPs deriving from aligned RAD-loci in a dataset consisting of 11

admixed individuals, 8 *An. nili* parents and 15 *An. ovengensis* parents. We calculated average values of α and β across five runs of *bgc*, each run including 50000 steps with samples from the posterior distribution recorded every 25th step following a 25000 step burn-in. We visually inspected the MCMC output to assess convergence to the stationary distribution.

To examine the relationship between the strength of selection and introgression, we tested whether loci with extreme or outlier genomic clines were enriched in genomic regions that were targets of selection. To do so, we studied the correlation between locus-specific cline parameters (α and β) and several divergence and diversity statistics (F_{ST}, d_{xy}, θ_w, θ_π, Tajima's D) across 9622 SNPs in the genome. The strength of correlation was assessed using Pearson's product moment correlation coefficient.

Results

SNP genotyping

We collected mosquitoes from four locations (Fig. 1A, Table S1) and sequenced 145 individuals belonging, according to morphological identifications and PCR, to two species (*An. nili* (n = 24) and *An. ovengensis* (n = 121)). We aligned reads from all 145 individuals to the reference genome and we assembled 197724 96-bp RAD loci that mapped to unique positions throughout the genome. We retained 408 loci present in all populations and in at least 50% of individuals in each population and identified 4343 high-quality biallelic markers within these loci. We also identified another set of 704408 unique loci by building consensus RAD loci *de novo* without aligning reads to the reference genome. We applied the same stringent filtration as with aligned reads to identify 3071 high-quality SNPs.

Genetic structure of populations

PCA and NJ trees showed that the genotype variation at 4343 genome-wide SNPs among the 145 sequenced individuals is best explained by more than two clusters, implying cryptic subdivisions among *An. nili* and *An. ovengensis* populations (Fig. 1C-D). The first three PCA axes and NJ trees clearly distinguished three subgroups within *An. nili* and two clusters in *An. ovengensis*. The five different clusters were associated with the sampling locations suggesting a strong correlation between the genetic structure and a local distinctness of populations. This marked geographic structure of *An. nili* and *An. ovengensis* populations can be explained by the ongoing adaptive divergence and ecological speciation within the two species. Importantly, both STRUCTURE and ADMIXTURE analyses revealed that, at k = 3, a subgroup containing 11 individuals corresponded to a cluster of hybrids with almost

half ancestry from *An. nili* and half from *An. ovengensis* (Fig. 1B). This result is surprising given the substantial time since divergence. We applied three different methods to identify the optimal number of genetic clusters in our samples. The DAPC suggested the presence of five clusters as indicated by PCA and NJ trees (Fig. 1E). However, the method of Evanno et al. indicated two probable ancestors while the distribution of the cross-validation error as a function of the number of putative populations in ADMIXTURE failed to unambiguously reveal an optimal number of genetic clusters (Fig. 1F,G). These conflicting results between methods are sometimes observed when the history of subdivisions and admixtures events is very complex as it is the case in *An. nili s.l* (Decker *et al.* 2014). The Evanno et al. method is overwhelmed by early divergence between *An. nili* and *An. ovengensis* while the results of DAPC and the ADMITURE cross-validation error reflect recent hierarchical population subdivisions within the two species. The inferred genetic structure was consistent when we used respectively 4343 and 3071 SNPs identified from reference-based and *de novo* assemblies (Fig. 1 and Fig. S1).

Genetic differentiation

We estimated the level of population differentiation between the five genetic clusters identified in our samples using the overall pairwise F_{ST} (Table 1). We found strong pairwise differentiation characterized by extreme F_{ST} values, including between populations classified as belonging to the same species. The level of differentiation is even higher between some pairs of populations within the same species than between *An. nili* and *An. ovengensis*. The highest level of within-species genetic differentiation was recorded between "allopatric" populations of *An. ovengensis* collected from locations separated by

~350km (F_{ST} = 0.896, p < 0.005). These findings strongly suggest that, in addition to hybridization, local differentiation associated with late stages of adaptive divergence within species are overwhelming current taxonomic descriptions in *An. nili s.l.* populations. The results obtained with reference alignments perfectly mirrored those of *de novo* assemblies (Table 1, S2). Taken as a whole, the population genetic structure and divergence of *An. nili* and *An. ovengensis* depicts a radiating group involving a collection of species whose phylogenetic relationships are blurred by ongoing hybridizations. As a result, current taxonomic classifications based on morphological characters and point mutations on the ribosomal DNA cannot effectively describe the actual reproductive units and the vectorial capacity within the *An. nili* species group.

Evidence for recent gene flow between *An. nili* and *An. ovengensis*

We used *TreeMix* to construct a tree connecting the five species and to effectively describe and visualize the mixture(s) event(s). The consensus of 100 ML *TreeMix* tree inferred from 4343 SNPs without migration resumes population-level relationships described by neighbor-joining analysis, PCA and clustering analyses (Fig. 2A). The long terminal branches leading to *An. nili* group 1, *An. nili* group 2 and *An. ovengensis* group 1 in the inferred tree reflect the signatures of strong bottlenecks in the history of these species. Interestingly, the residual fit from the ML model without migration suggested some correlations between species that were consistent with the admixture events inferred from ADMIXTURE and STRUCTURE analyses, particularly between the two species *An. nili* group 2 and *An. ovengensis* group 2 (Fig. 1B). Additional support to admixture was provided by the four-population test. Across all possible combinations of populations, there was a highly

334 significant allele frequency correlation between *An. nili* group 2 and *An. ovengensis* group 1
335 confirming that *An. nili* group 1 is the result of an admixture event between *An. nili* group 2
336 and *An. ovengensis* group 1 (Table 2 and S3). Nevertheless, five independent runs of *TreeMix*
337 including one or two migrations edges captured none of these migration events. Also, the
338 explained variance of the *TreeMix* ML model without migration edge was very high (99.8%)
339 indicating that a bifurcation tree can also match the phylogenetic relationships among
340 sampled populations. Finally, we found no significant f_3 statistics in all triplets of
341 populations, but this test may be underpowered because of the low-level and the precocity
342 of admixture or because of the complex demographic history of our populations (Decker *et*
343 *al.* 2014). As we showed previously with the population structure and genetic divergence,
344 the admixture events we described between *An. nili* and *An. ovengensis* also hold across
345 assembly methods (*de novo* or reference alignments)(Fig. 2 and S2).

346 **Genomic signatures of divergent selection and differential introgression**

347 We retained 9622 SNP loci identified from a reference-based assembly that we used to
348 examine the genomic footprints of divergent selection and introgression in a dataset
349 containing 8 "pure" *An. nili s.s.* individuals, 15 "pure" *An. ovengesis* and 11 admixed
350 individuals (see Materials and methods). The values of F_{ST} among SNP loci between parent
351 species *An. nili* and *An. ovengensis* were heterogeneous across the genome (Fig. 3). The
352 empirical distribution of locus-specific F_{ST} also revealed an unusually bimodal shape
353 featuring F_{ST} peaks centered on values around 0 and 1. The great majority of sites have low
354 to moderate differentiation, but a substantial number of loci are extremely differentiated
355 between the two species (Fig. 3A). We thinned our SNP set to 4003 using more stringent

356 filtration criteria and identified 42 statistical outliers of F_{ST} in LOSITAN, which were all
357 above the 99th percentile of the empirical distribution of F_{ST}. The bimodality of the genetic
358 divergence between *An. nili* and *An. ovengensis* is also evident in the empirical distribution
359 of d_{xy} (Fig. 3B). As exemplified by some empirical cases like the introgressive hybridization
360 observed between two closely related species of monkeyflowers (*Mimulus*) (Brandvain *et*
361 *al.* 2014), the bimodal divergence is due to the coexistence between sites of abrupt
362 differentiation reflecting the real level of divergence between the two species and sites of
363 low divergence resulting from recent gene flow. We conducted Linkage Disequilibrium (LD)
364 analyses to understand if highly differentiated sites are clustered into blocks of linked loci
365 or dispersed throughout the genome. Particularly, polymorphic chromosomal inversions
366 are important sources of genetic variation in *Anopheles* species and play a key role in local
367 adaptation and speciation. High F_{ST} values can aggregate in genomic regions containing
368 chromosomal inversions polymorphisms that are under strong divergent selection and
369 drive adaptive segregation as often observed in other African anopheline mosquitoes
370 (Ayala *et al.* 2011; Cheng *et al.* 2012; Kamdem *et al.* 2016). Cytogenetic studies have
371 detected no polymorphic chromosomal inversion among *An. ovengensis* samples. Two
372 polymorphic inversions (2*Rb*, 2*Rc*) have been identified in *An. nili*, but samples from
373 Cameroon bore only the 2*Rc* at a low frequency (Sharakhova *et al.* 2013). Rearranged
374 regions of the genome are characterized by reduced recombination and increased LD
375 relative to the genome-wide average. To effectively examine the extent of LD in the
376 genomes of *An. nili* and *An. ovengensis* and to test for the effect of chromosomal inversion
377 polymorphisms in adaptive evolution, we used the package LDna to identify clusters of LD.

To prevent spurious clusters due to LD between SNPs located on the same RAD locus, we used a dataset in which only one SNP was randomly selected within each RAD locus (1330 SNPs in total). We optimized LDna clustering parameters, which indicated the presence of 6 LD blocks (Single Outlier Clusters (SOCs)) among our samples (Fig. 4). These clusters represent signals of independent or compound events in the evolutionary history that left imprints on LD across the genome (Kemppainen *et al.* 2015). To further understand the role of the 6 LD clusters in the evolutionary history of *An. nili* and *An. ovengensis*, we conducted downstream analysis using PCA to examine the population structure of SNPs within each SOC. We found that one SOC (containing 39 SNPs) clearly discriminated a cluster encompassing all hybrid individuals from the two parent species (Fig. 4B). Two other SOCs (containing respectively 383 and 112 SNPs) consistently separated one parent species from a group comprising the other parent species and all hybrid individuals. The last three SOCs revealed no clear clustering patterns. None of the SOCs differentiated clusters that could be associated with the three alternative karyotypes (inverted homozygotes, heterozygotes and uninverted homozygotes) expected in case of polymorphic inversion. As suggested by cytogenetic observations, polymorphic inversions likely play only a moderate role in the genomic divergence in *An. nili s.l,* but a more intensive sampling is needed to make any definitive conclusion. Interestingly, the three most important blocks of LD found in the genomes of *An. nili* and *An. ovengensis* are instead associated with hybridization, which emphasizes the central role played by interspecific gene flow in the genomic architecture of adaptive speciation in the two species. Our results also suggest that loci resistant to introgression and genes responsible for reproductive isolation between *An. nili* and *An.*

400 *ovengensis* are in strong linkage disequilibrium. This finding is consistent with recent
401 introgression whereby long-range haplotypes that are generated by recent gene flow
402 between genetically distinct populations have not have sufficient time to be broken down
403 by recombination (admixture-induced LD) (Martin *et al.* 2013). However, LDna estimates
404 the LD irrespective of the physical linkage between markers and LD blocks can also result
405 from a strong correlation between allelic frequencies of SNPs scattered throughout the
406 genome. A detailed characterization of long-range haplotypes across genomes of *An. nili* and
407 *An. ovengensis* will provide a more powerful examination of the genomic architecture of
408 reproductive isolation between the two species.
409 Here we have used another innovative approach (genomic cline) to further understand the
410 relationship between divergence, selection and differential introgression at the genomic
411 level. First, consistent with STRUCTURE and ADMIXTURE results, the empirical distribution
412 of hybrid index among admixed individuals (average hybrid index ~0.3) shows a slight
413 predominance of *An. ovengensis* ancestry (Fig. 5A, Fig. 1B). Using estimates of genomic cline
414 parameters, we noted that introgression was very heterogeneous across loci (Fig. 5B).
415 Indeed, the level of introgression at 1297 SNP loci differed significantly from the genome-
416 wide average (outliers) and we detected an excess *An. ovengensis* ancestry for 2506 loci
417 (lower bound of 95% CI for $\alpha > 0$) and excess *An. nili* ancestry for 2635 loci (upper bound of
418 95% CI for $\alpha < 0$). Estimates of the genomic cline parameter α range from -5 to 5.25 while
419 our values of β are low overall (β varies from -0.13 to 0.09). Moreover, we identified no loci
420 with significantly elevated estimates of genomic cline rate. The β parameter assesses the
421 rate of transition from one ancestry to the other and thereby scores the steepness of the

422 genomic cline at each locus. Extreme values of β are expected when there is population
423 structure in the hybrid zone, selection against hybrids or gene flow among parent species
424 (Parchman *et al.* 2013). Our hybrid population is highly differentiated (F_{ST} > 0.8) from both
425 parent species and is well adapted in hybrid zone, which certainly explain the low β values
426 observed. One key aspect in the Bayesian implementation of genomic clines is the
427 relationship between α and β, which is crucial to understand the rate of transition of sites of
428 exceptional introgression from one side to the other of the genome. As we have shown
429 previously with F_{ST} and d_{xy}, recent introgression in divergent genomes of *An. nili* and *An.*
430 *ovengensis* has resulted in bimodal genomic divergence featuring two blocks of sites with
431 extreme divergence values. This pattern presumes that most variant sites will have very
432 steep genomic clines because the transition from one ancestry to the other is very abrupt.
433 In agreement with this prediction, the scatterplot of β as a function of α indicates the
434 presence of two blocks of SNPs with either high probability of *An. nili* or of *An. ovengensis*
435 ancestry (Fig. 5B). The genomes of both species are split into two compartments of ancestry
436 due to recent introgression resulting in steep genomic clines at hybrid zone (Fig. 5B). To
437 better understand the biological significance of these outlier loci of introgression in
438 admixed individuals, we assessed the correlation between α and β and locus-specific
439 estimates of divergence and selection parameters. We found a detectable negative
440 correlation between F_{ST} and values of α ($r = -0.15$, $p < 0.005$). Among the 32 LOSITAN F_{ST}
441 outliers, 13 loci had extreme α estimates, and 11 were outlier of β, but the average values of
442 both α and β were not significantly different between F_{ST} outliers and the 9622 genome-
443 wide SNP loci (Mann-Whitney U-test, $P < 0.001$). Erroneous correlation between F_{ST} and

444 exceptional introgression can inferred when the F_{ST} between parental populations is < 0.1
445 (Parchman *et al.* 2013). The high overall F_{ST} (~0.8) between *An. nili* and *An. ovengensis*
446 minimizes such errors in our study. We also detected a negative correlation between α and
447 d_{xy} (r = -0.13, p < 0.005), which confirms previous results with F_{ST}, suggesting that sites that
448 diverge strongly resist to differential introgression because they likely contain reproductive
449 isolation factors. The negative correlation between d_{xy} and estimates of locus-specific
450 admixture indicates that perhaps gene flow has had sufficient time to reduce sequence
451 divergence at admixed loci despite the relatively recent hybridization process. We next
452 correlated cline parameters (α and β) to the estimates of locus-specific diversity (θ_w and θ_π
453) and the allele frequency spectrum (Tajima's *D*). The results provided another clear
454 illustration of the steep genomic clines described previously with alpha and beta values.
455 Notably, there is a strong positive correlation between θ_w and α (r = 0.53, p< 0.005) in *An.*
456 *ovengensis* and a negative correlation of the same magnitude with the diversity of *An. nili* (r
457 = -0.49, p< 0.005), which translate the segregation of genomes of admixed individuals in
458 two sources of ancestry that are at opposite ends of the genomic cline. Interestingly, the
459 high correlation between alpha and diversity indicate that sites that are favored by
460 introgression are not constrained by divergent selection that should have likely resulted in
461 depression in nucleotide diversity. In contrast to what has been shown in manakin birds
462 (Parchman *et al.* 2013) and in *Lycaeides* butterflies (Gompert *et al.* 2012, 2013), there is no
463 evidence of increased introgression at loci under divergent selection between *An. nili* and
464 *An. ovengensis*.

Discussion

Hybridization at late stages of speciation

We have described a complex case of speciation and hybridization in a group of related *Anopheles* mosquitoes endemic to Sub-Saharan Africa. Both incomplete speciation and pervasive hybridization are leading to a very dynamic pattern of genetic structure between and within species. We first analysed the population genetic structure and revealed cryptic subdivisions between the two malaria vectors *An. nili* and *An. ovengensis*. The exact number of demes or cryptic subgroups within each species in our samples was difficult to determine. We found conflicting results between estimates from three different genetic clustering methods. However, three different methods suggested the existence of 2 to 5 clusters in our sample. *An. nili* is subdivided into three clusters while ongoing adaptive speciation in *An. ovengensis* results so far in two cryptic species. The extremely high genetic differentiation between populations indicates that all these cryptic subgroups are almost complete species. Our results therefore suggest that *An. nili* and *An. ovengensis,* contrary to the current taxonomy, represent probably two different complexes of cryptic species. The geographic origin of samples explains a great part of the genetic variance among individuals consistent with strong local differentiation and adaptive speciation. Significant population structure has been described among *An. nili* populations from Cameroon with 8 microsatellite loci (Ndo *et al.* 2013). Ndo *et al*. 2013 also found F_{ST} values as high as 0.48 between two populations from the forest area. Using genome-wide SNPs, we have identified new subdivisions and revealed that the population genetic structure of *An. nili* is more complex. Our work highlights the strength of Next Generation Sequencing (NGS)

487 approaches and the necessity of fine-scale genomic examinations in the resolution of
488 intricate patterns of ancestry in this group of mosquito. By contrast, the ongoing speciation
489 we have observed within *An. ovengensis* has never been described in the past, and this
490 species has been sometimes considered as a sibling of *An. nili* (Kengne *et al.* 2003; Awono-
491 Ambene *et al.* 2004, 2006; Ndo *et al.* 2013). Nevertheless, more recent studies have started
492 to challenge the assumed relatedness between the two species (Ndo *et al.* 2013; Sharakhova
493 *et al.* 2013). Precisely, analyses of polytene chromosomes revealed high karyotypic
494 divergence of *An. ovengensis* from *An. nili* (Sharakhova *et al.* 2013) and estimates of time
495 since divergence indicated that the two species split from one another 3 to 6-Myr ago (Ndo
496 *et al.* 2013). Intriguingly, our work provides multiple lines of evidence supporting the
497 existence of extensive ongoing gene flow between the two species despite this strong
498 divergence. First, clustering methods and Bayesian implementation of genomic clines
499 identified individuals with almost half ancestry from both species and formal tests of
500 population admixture corroborated these ongoing admixture events. Second, perhaps the
501 most compelling evidence for hybridization is the presence of admixture-induced linkage
502 disequilibrium (ALD) characterized by blocks of linked SNPs that discriminate hybrid
503 populations from parental species. In general, linkage disequilibrium (LD) or the
504 correlation between allele frequencies of different loci across the genome, which can have
505 multiple origins including selection, genetic drift, or population structure, is normally
506 eroded by recombination in the course of time. ALD is caused by associations between
507 nearby loci co-inherited on an intact chromosomal block from one of the ancestral mixing
508 populations (Loh *et al.* 2013). Signatures of ALD are frequent in genomes of recently

admixed populations for which recombination has not yet broken the large introgressed chromosomal segments into smaller portions. ALD is a well-known feature in evolutionary history of humans and estimates of long-range LD have been proposed as an approach to measure the extent and the timing of admixture events that have shaped the genetic polymorphism across genomes of extant populations (Loh *et al.* 2013). In insects, signatures of ALD have been found for example in the *Heliconius* butterfly genome, especially around loci involved in mimicry of color patterns that circulate between species (Martin *et al.* 2013). *An. nili* provides another rare example of ALD across the genome of an insect species. Further studies using a more comprehensive genomic sequencing and a reference genome of better quality will help us to improve our knowledge of functional and sequential characteristics of admixed LD blocks found in the *An. nili* genome.

Although the concept of speciation-with-gene-flow has become the dominant paradigm in speciation studies, we remain ignorant about the conditions that prevent or motivate gene flow between divergent lineages before the onset of complete reproductive isolation. Moreover, even the notion of "complete reproductive isolation" is now challenged because an increasing number of examples from diverse taxa showed rampant gene exchange across strong reproductive barriers, sometimes between established species that diverged several million years ago (Nydam & Harrison 2011; Roux *et al.* 2013; Parchman *et al.* 2013; Martin *et al.* 2013; Canestrelli *et al.* 2014). These studies and ours suggest that processes underlying hybridization and introgression in the presence of clear genetic differentiation will be best addressed within speciation continuum rather than across couples of occasionally mating species. A continuum of speciation featuring a collection of taxa

531 occupying a gradient of genetic/ecological divergence provides ideal conditions where the
532 relation between divergence and hybridization can be inferred. Contrary to what we
533 initially thought, the *An. nili* group does not represent a speciation continuum but instead a
534 collection of complete species sharing a common ancestry. Moreover, despite extensive
535 efforts, we couldn't sample populations of the two remaining species of the group: *An.*
536 *somalicus* and *An. carnevalei*. Therefore, patterns of admixtures and ancestry among
537 populations of this group of mosquitoes are probably more complex than what we have
538 shown. Nevertheless, instead of a comprehensive description of splits and admixtures in *An.*
539 *nili s.l.*, we have focused our efforts on the examination of the genomic architecture of
540 divergence and introgression between *An. nili* and *An. ovengensis.* The results we discuss
541 below are among the rare cases that address the genomic signatures of gene flow and the
542 relationship between divergence, selection and introgression at late stages of the speciation
543 process.

544 **Genomic architecture of adaptive introgression**

545 Owing to the increasing availability of high-throughput sequencing information, genomes of
546 multiple taxa have been scanned and analyzed in comparative frameworks to search for
547 genomic signatures of divergence and speciation. The prevailing idea behind these
548 approaches is that regions of extreme differentiation between incipient or complete species
549 contain factors that maintain reproductive isolation (RI) among their populations. In
550 reality, the genomic distribution of highly differentiated regions has been more contentious
551 (Nosil & Feder 2012, 2013). Overall, two models are well documented: the "speciation
552 island" model whereby RI loci are thought to be caught up in in a few regions of the genome

553 where outliers of genetic differentiation cluster (e.g. (Andrew & Rieseberg 2013)) and the
554 "heterogeneous" distribution model, which posits that genomic divergence is instead lead
555 by numerous small genomic regions scattered throughout all chromosomes (e.g.
556 (Lawniczak *et al.* 2010; Roesti *et al.* 2012)). A shift in this paradigm is envisioned as
557 evidence is accumulating indicating that highly differentiated loci can paradoxically
558 coincide with regions of elevated introgression between two species (Gompert *et al.* 2012,
559 2013; Pool *et al.* 2012; Parchman *et al.* 2013). The genomic distribution of the genetic
560 divergence between *An. ovengensis* and *An. nili* shows that the compound effects of strong
561 divergence and recent introgression generates a bimodal pattern of divergence which
562 assigns most sites into two main categories: a majority of low divergence sites and a small
563 cluster of high divergence loci with F_{ST} values centered around 1. In most of the widespread
564 *Anopheles* species, signatures of high divergence can be found in large chromosomal
565 segments corresponding to rearranged regions of chromosomes where recombination is
566 rare (Neafsey *et al.* 2015). This is the case for example in the 2L*a* inversion locus, which
567 depicts signatures of strong divergent selection along a latitudinal cline (Cheng *et al.* 2012).
568 In agreement with cytogenetic studies, which found roughly no polymorphic inversions
569 among *An. nili* samples from Cameroon, we observed no tendency for high F_{ST} or d_{xy} to
570 cluster within regions that can be assimilated to chromosomal rearrangements. In contrast
571 to what has been recently demonstrated in manakin birds (Parchman *et al.* 2013) and in
572 *Lycaeides* butterflies (Gompert *et al.* 2012, 2013), there is a negative correlation between
573 the introgression parameter α and genetic divergence (estimated both as F_{ST} an d_{xy})
574 between *An. nili* and *An. ovengensis*. As expected, gene flow is favored across neutral loci

575 and those that provide selective advantage, but are presumably not under strong divergent
576 selection. Moreover, the relationship between α and β suggests a prevalence of steep clines
577 in genomes of admixed individuals at contact zones. This also translates into a positive
578 correlation between α and the nucleotide diversity in *An. ovengensis* and a negative
579 correlation of α to the diversity of *An. nili*. In theory, SNPs with steep cline are hypothesized
580 to be near genes involved in reproductive isolation and as such are possibly under selection
581 in hybrids (Janoušek *et al.* 2015). Therefore, the abundance of steep clines provides another
582 clear illustration of the mosaic genome characterized by coexistence between high
583 divergence and consistent gene flow observed in the hybrid species.
584 A substantial body of evidence indicates that genomic material coming from related species
585 can confer an advantage to populations (adaptive introgression). Adaptive introgression of
586 one or two loci has been widely studied over the last two decades and excellent examples
587 have been described. The most prominent cases include the transfer of genes involved in
588 mimicry of color patterns in *Heliconius* butterflies (Consortium 2012), the circulation of
589 resistant alleles of insecticides in mosquitoes (Clarkson *et al.* 2014; Norris *et al.* 2015) and
590 rodenticide in mice (Song *et al.* 2011). However, although convincing signatures of adaptive
591 introgression around one gene or a few linked loci can now be described in an increasing
592 number of species, the extent and the magnitude of introgressive hybridization across the
593 genome remained unknown. Further, due in part to the fact that most species in which the
594 concomitance of introgressive hybridization and high divergence has been observed are
595 nonmodel species with little genomic resources, the knowledge of genomic characteristics
596 of adaptive introgression in these species remains relatively modest. Meanwhile, a

consistent pattern has started to emerge from the few cases that have been studies with substantial genomic details. In general, genomic regions exhibiting non-random introgression are widely dispersed across the genome, rather than co-localized in a few discrete blocks. This heterogeneity of genome-wide introgression patterns has been observed for example between manakin birds (*Manacus candei* and *M. vitellinus*) (Parchman *et al.* 2013) in different mice subspecies (Liu *et al.* 2015), and among mosquitoes of the *Anopheles gambiae* species complex (Fontaine *et al.* 2014; Kamdem *et al.* 2016). Our results also show that selective introgression can be widespread across the genome of two highly divergent species. However, in contrast to most of the reference cited, LD analyses in *An. nili* and *An. ovengensis* have revealed a LD cluster separating hybrids from the two parental species, which suggests that at least some of the recently introgression loci consist of relatively large chromosome segments that have yet to be further characterized sequentially and functionally with a high-quality reference genome. In addition to the lack of knowledge about the genomic architecture, the functional and phenotypic aspects of introgressive hybridization between established species remain obscures. In mice for example, introgression is associated with a polarization of GO terms, regions of elevated introgression exhibiting a disproportionate number of genes involved in signal transduction and olfactory receptor genes (Janoušek *et al.* 2015). Hybrids between *An. nili* and *An. ovengensis* were collected from an area of the equatorial forest whose environmental features were not apparently very divergent from those of the locations where the parent species were sampled (Fig. 1A). As a result, it is hard to pinpoint

618 environmental gradients and the life history traits that can be considered as the main
619 drivers of speciation and introgression among species of *An. nili* and *An. ovengensis*.
620

621 **Conclusions and implications**

622 Although hybridization has been recognized as one of the major forces that affect the
623 evolution of living species, the detailed study of its fundamental and applied implications
624 has been hampered by methodological limitations. Advances in high-throughput DNA
625 sequencing and statistical genomics are revolutionizing experimental and conceptual
626 approaches, allowing a very sensitive examination of the heterogeneity of hybridization
627 across species and genomes. We have used a combination of tests tailored to infer patterns
628 of introgression across genomes of nonmodel species. Although our results still need to be
629 replicated in other contact zones across the distribution range of *An. nili* in Africa, they
630 highlight the complex relationships between divergence, selection and introgression during
631 the split of taxa. Our work has methodological, conceptual and applied implications. Most
632 genome scans assume a negative correlation between genetic divergence and introgression.
633 It has been suggested that that the opposite is possible (Parchman *et al.* 2013; Gompert *et*
634 *al.* 2013), but our findings do no support this hypothesis. Climate change and anthropogenic
635 disturbance are contributing to expand geographic ranges of mosquito species worldwide
636 thereby increasing contact between previously isolated species that are capable of
637 exchanging gene flow. This interspecific gene flow in mosquitoes often leads to the spread
638 of insecticide resistance alleles and other epidemiologically significant genes. Our work
639 provided a methodological validation of a cost-effective population genomic approach that
640 can be applied to investigate the bases of introgressive hybridization in other mosquito
641 species.
642

Acknowledgements

Funding for this project was provided by the University of California Riverside and NIH grants 1R01AI113248 and 1R21AI115271 to BJW.

References

Abbott R, Albach D, Ansell S *et al.* (2013) Hybridization and speciation. *Journal of Evolutionary Biology*, **26**, 229–246.

Alexander DH, Novembre J, Lange K (2009) Fast model-based estimation of ancestry in unrelated individuals. *Genome Research*, **19**, 1655–1664.

Andrew RL, Rieseberg LH (2013) Divergence is focused on few genomic regions early in speciation: incipient speciation of sunflower ecotypes. *Evolution; international journal of organic evolution*, **67**, 2468–82.

Antonio-Nkondjio C, Kerah CH, Simard F *et al.* (2006) Complexity of the malaria vectorial system in Cameroon: contribution of secondary vectors to malaria transmission. *Journal of medical entomology*, **43**, 1215–1221.

Antonio-Nkondjio C, Ndo C, Costantini C *et al.* (2009) Distribution and larval habitat characterization of Anopheles moucheti, Anopheles nili, and other malaria vectors in river networks of southern Cameroon. *Acta Tropica*, **112**, 270–276.

Awono-Ambene HP, Kengne P, Simard F, Antonio-Nkondjio C, Fontenille D (2004) Description and bionomics of Anopheles (Cellia) ovengensis (Diptera: Culicidae), a new malaria vector species of the Anopheles nili group from south Cameroon. *Journal of medical entomology*, **41**, 561–568.

Awono-Ambene HP, Simard F, Antonio-Nkondjio C *et al.* (2006) Multilocus enzyme electrophoresis supports speciation within the Anopheles nili group of malaria vectors in Cameroon. *The American journal of tropical medicine and hygiene*, **75**, 656–658.

Ayala D, Fontaine MC, Cohuet A *et al.* (2011) Chromosomal inversions, natural selection and adaptation in the malaria vector Anopheles funestus. *Molecular biology and evolution*, **28**, 745–758.

Beaumont MA, Nichols RA (1996) Evaluating loci for use in the genetic analysis of population structure. *Proceedings of the Royal Society B: Biological Sciences*, **263**, 1619–1626.

Brandvain Y, Kenney AM, Flagel L, Coop G, Sweigart AL (2014) Speciation and Introgression between Mimulus nasutus and Mimulus guttatus. *PLoS Genetics*, **10**.

Canestrelli D, Bisconti R, Nascetti G (2014) Extensive unidirectional introgression between two salamander lineages of ancient divergence and its evolutionary implications. *Scientific reports*, **4**, 6516.

Cheng C, White BJ, Kamdem C *et al.* (2012) Ecological genomics of Anopheles gambiae along a latitudinal cline: a population-resequencing approach. *Genetics*, **190**, 1417–32.

Clarkson CS, Weetman D, Essandoh J *et al.* (2014) Adaptive introgression between Anopheles sibling species eliminates a major genomic island but not reproductive isolation. *Nature communications*, **5**, 4248.

Consortium THG (2012) Butterfly genome reveals promiscuous exchange of mimicry adaptations among species. *Nature*, **487**, 94–8.

Decker JE, McKay SD, Rolf MM *et al.* (2014) Worldwide Patterns of Ancestry, Divergence, and Admixture in Domesticated Cattle. *PLoS Genetics*, **10**.

Earl DA, VonHoldt BM (2012) STRUCTURE HARVESTER: a website and program for visualizing STRUCTURE output and implementing the Evanno method. *Conservation*

692 *Genetics Resources*, **4**.
693 Ellegren H, Smeds L, Burri R *et al.* (2012) The genomic landscape of species divergence in
694 Ficedula flycatchers. *Nature*, **491**, 756–60.
695 Evanno G, Goudet J, Regnaut S (2005) Detecting the number of clusters of individuals using
696 the software structure: a simulation study. *Molecular Ecology*, **14**, 2611–2620.
697 Fontaine MC, Pease JB, Steele A *et al.* (2014) Extensive introgression in a malaria vector
698 species complex revealed by phylogenomics. *Science*, **347**, DOI:
699 10.1126/science.1258524.
700 Fumagalli M, Vieira FG, Linderoth T (2014) ngsTools : methods for population genetics
701 analyses from Next-Generation Sequencing data. *Bioinformatics*.
702 Gillies MT, Coetzee M (1987) *A supplement to the Anophelinae of Africa south of the Sahara*.
703 The South African Institute for Medical Research, Johannesburg.
704 Gillies MT, De Meillon B (1968) *The Anophelinae of Africa South of the Sahara*. Publications
705 of the South African Institute for Medical Research, Johannesburg.
706 Gompert Z, Alex BC (2011) Bayesian estimation of genomic clines. *Molecular ecology*, **20**,
707 2111–2127.
708 Gompert Z, Buerkle C a. (2012) <tt>bgc</tt> : Software for Bayesian estimation of genomic
709 clines. *Molecular Ecology Resources*, **12**, 1168–1176.
710 Gompert Z, Lucas L, Nice C (2012) Genomic regions with a history of divergent selection
711 affect fitness of hybrids between two butterfly species. …, 2167–2181.
712 Gompert Z, Lucas LK, Nice CC, Buerkle CA (2013) Genome divergence and the genetic
713 architecture of barriers to gene flow between Lycaeides idas and L. Melissa. *Evolution;*
714 *international journal of organic evolution*, **67**, 2498–514.
715 Grant BR (2015) Introgressive hybridization and natural selection in Darwin's finches.
716 *Biological Journal of the Linnean SocietyBiolog*, 812–822.
717 Hohenlohe P a, Bassham S, Etter PD *et al.* (2010) Population genomics of parallel adaptation
718 in threespine stickleback using sequenced RAD tags. *PLoS genetics*, **6**, e1000862.
719 Jakobsson M, Rosenberg N (2007) CLUMPP: a cluster matching and permutation program
720 for dealing with multimodality in analysis of population structure. *Bioinformatics*, **23**,
721 1801– 1806.
722 James M (2007) Hybrid speciation. *Nature*, **446**, 279–283.
723 Janoušek V, Munclinger P, Wang L, Teeter KC, Tucker PK (2015) Functional organization of
724 the genome may shape the species boundary in the house mouse. *Molecular Biology*
725 *and Evolution*, **32**, 1208–1220.
726 Jombart T (2008) adegenet: a R package for the multivariate analysis of genetic markers.
727 *Bioinformatics*, **24**, 1403–1405.
728 Kamdem C, Fouet C, Gamez S, White BJ (2016) Pollutants and insecticides drive local
729 adaptation in African malaria mosquitoes. *bioRxiv*.
730 Kemppainen P, Knight CG, Sarma DK *et al.* (2015) Linkage disequilibrium network analysis
731 (LDna) gives a global view of chromosomal inversions, local adaptation and geographic
732 structure. *Molecular Ecology Resources*, n/a–n/a.
733 Kengne P, Awono-Ambene, H. P. Antonio-Nkondjio C, Simard F, Fontenille D (2003)
734 Molecular identification of the Anopheles nili group African malaria vectors. *Med Vet*
735 *Entomol*, **17**, 67–74.

736 Korneliussen T, Albrechtsen A, Nielsen R (2014) ANGSD: Analysis of Next Generation
737 Sequencing Data. *BMC Bioinformatics*, **15**, 356.
738 Lawniczak MKN, Emrich SJ, Holloway a K *et al.* (2010) Widespread divergence between
739 incipient Anopheles gambiae species revealed by whole genome sequences. *Science*
740 *(New York, N.Y.)*, **330**, 512–4.
741 Liu KJ, Steinberg E, Yozzo A *et al.* (2015) Interspecific introgressive origin of genomic
742 diversity in the house mouse. *Proceedings of the National Academy of Sciences*, **112**,
743 196–201.
744 Loh PR, Lipson M, Patterson N *et al.* (2013) Inferring admixture histories of human
745 populations using linkage disequilibrium. *Genetics*, **193**, 1233–1254.
746 Mallet J, Besansky N, Hahn MW (2015) How reticulated are species? *BioEssays*, 140–149.
747 Martin SH, Dasmahapatra KK, Nadeau NJ *et al.* (2013) Genome-wide evidence for speciation
748 with gene flow in Heliconius butterflies. *Genome research*, **23**, 1817–28.
749 Meirmans P, Van Tienderen P (2004) GENOTYPE and GENODIVE: two programs for the
750 analysis of genetic diversity of asexual organisms. *Molecular Ecology Notes*, **4**, 792–794.
751 Nadeau NJ, Martin SH, Kozak KM *et al.* (2013) Genome-wide patterns of divergence and
752 gene flow across a butterfly radiation. *Molecular ecology*, **22**, 814–26.
753 Ndo C, Antonio-Nkondjio C, Cohuet A *et al.* (2010) Population genetic structure of the
754 malaria vector Anopheles nili in sub-Saharan Africa. *Malaria journal*, **9**, 161.
755 Ndo C, Simard F, Kengne P *et al.* (2013) Cryptic Genetic Diversity within the Anopheles nili
756 group of Malaria Vectors in the Equatorial Forest Area of Cameroon (Central Africa).
757 *PLoS ONE*, **8**, 1–12.
758 Neafsey DE, Waterhouse RM, Abai MR *et al.* (2015) Highly evolvable malaria vectors: The
759 genomes of 16 Anopheles mosquitoes. *Science*, **347**, 1258522–1258522.
760 Norris LC, Main BJ, Lee Y *et al.* (2015) Adaptive introgression in an African malaria
761 mosquito coincident with the increased usage of insecticide-treated bed nets.
762 *Proceedings of the National Academy of Sciences*, 201418892.
763 Nosil P (2012) *Ecological Speciation*.
764 Nosil P, Feder JL (2012) Widespread yet heterogeneous genomic divergence. *Molecular*
765 *Ecology*, **21**, 2829–2832.
766 Nosil P, Feder JL (2013) Genome evolution and speciation: toward quantitative descriptions
767 of pattern and process. *Evolution; international journal of organic evolution*, **67**, 2461–
768 7.
769 Nydam ML, Harrison RG (2011) Introgression Despite Substantial Divergence in a
770 Broadcast Spawning Marine Invertebrate. *Evolution*, **65**, 429–442.
771 Ozerov MY, Gross R, Bruneaux M *et al.* (2016) Genome-wide introgressive hybridization
772 patterns in wild Atlantic salmon influenced by inadvertent gene flow from hatchery
773 releases. *Molecular Ecology*, n/a–n/a.
774 Paradis E, Claude J, Strimmer K (2004) Analyses of Phylogenetics and Evolution in R
775 language. *Bioinformatics*, **20**, 289–290.
776 Parchman TL, Gompert Z, Braun MJ *et al.* (2013) The genomic consequences of adaptive
777 divergence and reproductive isolation between species of manakins. *Molecular ecology*,
778 **22**, 3304–17.
779 Payseur BA, Rieseberg LH (2016) A Genomic Perspective on Hybridization and Speciation.

780 *Molecular Ecology*, n/a–n/a.
781 Peery A, Sharakhova M V, Antonio-Nkondjio C *et al.* (2011) Improving the population
782 genetics toolbox for the study of the African malaria vector Anopheles nili:
783 microsatellite mapping to chromosomes. *Parasites & Vectors*, **4**, 202.
784 Peterson BK, Weber JN, Kay EH, Fisher HS, Hoekstra HE (2012) Double Digest RADseq: An
785 Inexpensive Method for De Novo SNP Discovery and Genotyping in Model and Non-
786 Model Species. *PLoS ONE*, **7**, e37135.
787 Pickrell JK, Pritchard JK (2012) Inference of Population Splits and Mixtures from Genome-
788 Wide Allele Frequency Data. *PLoS Genetics*, **8**.
789 Pool JE, Corbett-Detig RB, Sugino RP *et al.* (2012) Population Genomics of Sub-Saharan
790 Drosophila melanogaster: African Diversity and Non-African Admixture. *PLoS Genetics*,
791 **8**.
792 Pritchard JK, Stephens M, Donnelly P (2000) Inference of population structure using
793 multilocus genotype data. *Genetics*, **155**, 945–959.
794 Purcell S, Neale B, Todd-Brown K *et al.* (2007) PLINK: a toolset for whole-genome
795 association and population-based linkage analysis. *American Journal of Human*
796 *Genetics*, **81**.
797 Reich D, Thangaraj K, Patterson N, Price AL, Singh L (2009) Reconstructing Indian
798 population history. *Nature*, **461**, 489–494.
799 Roesti M, Hendry AP, Salzburger W, Berner D (2012) Genome divergence during
800 evolutionary diversification as revealed in replicate lake-stream stickleback population
801 pairs. *Molecular ecology*, **21**, 2852–62.
802 Rosenberg N (2004) DISTRUCT: a program for the graphical display of population
803 structure. *Molecular Ecology Resources*, **4**, 137–138.
804 Roux C, Tsagkogeorga G, Bierne N, Galtier N (2013) Crossing the species barrier: Genomic
805 hotspots of introgression between two highly divergent ciona intestinalis species.
806 *Molecular Biology and Evolution*, **30**, 1574–1587.
807 Sharakhova M V., Peery A, Antonio-Nkondjio C *et al.* (2013) Cytogenetic analysis of
808 Anopheles ovengensis revealed high structural divergence of chromosomes in the
809 Anopheles nili group. *Infection, Genetics and Evolution*, **16**, 341–348.
810 Song Y, Endepols S, Klemann N *et al.* (2011) Adaptive introgression of anticoagulant rodent
811 poison resistance by hybridization between old world mice. *Current Biology*, **21**, 1296–
812 1301.
813 Sukumaran J, Holder MT (2010) DendroPy: A Python library for phylogenetic computing.
814 *Bioinformatics*, **26**, 1569–1571.
815 Turner TL, Hahn MW, Nuzhdin S V. (2005) Genomic islands of speciation in Anopheles
816 gambiae. *PLoS Biology*, **3**, 1572–1578.
817 Weir BS, Cockerham CC (1984) Estimating F-statistics for the analysis of population
818 structure. *Evolution*, **38**, 1358–1370.
819 Wu TD, Nacu S (2010) Fast and SNP-tolerant detection of complex variants and splicing in
820 short reads. *Bioinformatics*, **26**, 873–881.
821

822 **Author contributions**

823 Conceived and designed the experiments: CK CF BJW. Performed the experiments: CK CF SG
824 BJW. Analyzed the data: CK CF BJW. Wrote the paper: CK CF BJW.
825

826 **Tables**
827
828 **Table 1**: Pairwise F_{ST} between *An. nili* and *An. ovengensis* populations. p < 0.005 for all
829 values.

F_{ST}	***An. nili* group 1**	***An. nili* group 2**	***An. nili* group 3**	***An. ovengensis* group 1**	***An. ovengensis* group 2**
***An. nili* group 1**	-				
***An. nili* group 2**	0.794	-			
***An. nili* group 3**	0.838	0.863	-		
***An. ovengensis* group 1**	0.655	0.834	0.873	-	
***An. ovengensis* group 2**	0.857	0.863	0.858	0.896	-

830

831 **Table 2**: Results of the most significant f_4 tests for gene flow.
832

Test	f_4 ± std err			Z-score	P-value
f_4(Oveng 1 ,Nili 3 ; Nili 2, Nili 1)	-0.03506	±	0.00287	-12.20	< 0.00001
f_4(Oveng 1, Nili 3 ; Nili 2, Oveng 2)	0.02241	±	0.00263	8.52	< 0.00001
f_4(Oveng 1, Oveng 2 ; Nili 3, Nili 1)	-0.05775	±	0.00355	-16.25	< 0.00001
f_4(Oveng 1, Oveng 2 ; Nili 2, Nili 1)	-0.03718	±	0.00292	-12.72	< 0.00001
f_4(Nili 3, Nili 1 ; Nili 2, Oveng 2)	-0.02272	±	0.00263	-8.63	< 0.00001

Oveng 1: *An. ovengensis* group 1 ; Oveng 2: *An. ovengensis* group 2 ; Nili 1: *An. nili* group 1 ; Nili 2: *An. nili* group 2 ; Nili 3: *An. nili* group 3

833

834 **Table 3**: Pearson's correlation coefficient assessing the relationship between cline
835 parameter (α and β) and locus-specific estimates of five population genomic parameters
836 (pairwise genetic divergence (F_{ST} and d_{xy}), nucleotide diversity (θ_w and θ_π) and allele
837 frequency spectrum (Tajima's *D*)).
838

	Hybrids							*An. nili*			*An. ovengensis*			
	F_{ST}	d_{xy}	θw		θπ		T*D*		θw	θπ	T*D*	θw	θπ	T*D*	
α	-0.151	-0.130	0.057		0.052		0.016	*	-0.498	-0.414	0.088	0.537	0.432	-0.033	*
β	0.060	0.048	-0.016	*	-0.017	*	-0.011	*	0.230	0.188	-0.047	-0.266	-0.212	0.018	*

* not significant (p>0.005)

T*D*: Tajima's *D*

Figures

Figure 1: Population genetic structure of *An. nili sensu lato* inferred from 4343 SNPs identified with a reference-based assembly. (A) Map showing the sampling locations and relative frequencies of the two *An. nili* and *An. ovengensis*. (B) ADMIXTURE plots with k from 2 trough 8. (C) and (D) neighbor-joining tree and PCA. Each PCA axis is labeled with the percentage of variance explained. (E), (F) and (G) Identification of the optimal number of genetic clusters using the delta k method of Evanno et al, DAPC, and 10-fold cross-validation in ADMIXTURE. The lowest BIC and CV error and the highest delta k indicate the most probable number of genetic clusters.

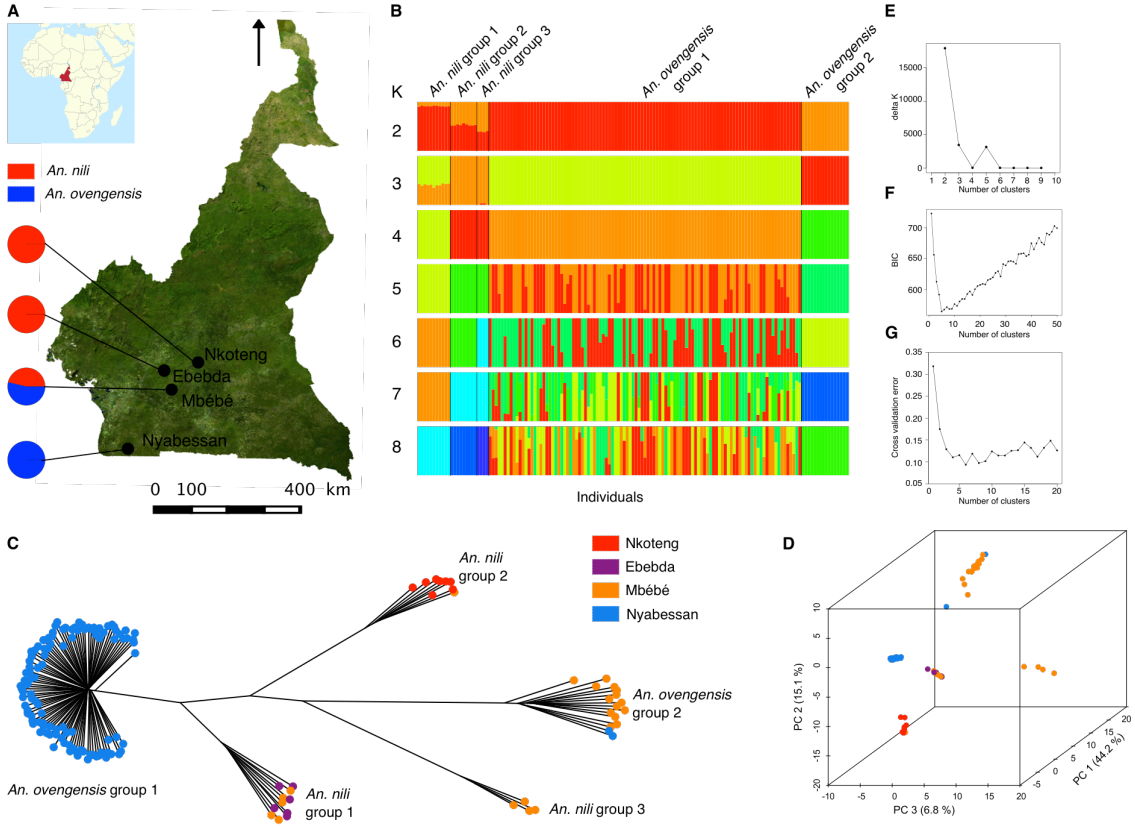

Figure 2. *TreeMix* Maximum Likelihood (ML) trees depicting the signals of gene flow between *An. nili* and *An. ovengensis*. ML tree and residual fit from the ML model inferred with (A) no migration edge, (B) a single migration edge and (C) two migration edges. The small arrow on each indicates the directionality of gene flow migration edge and the color of the edge reflect the intensity of admixture. Heat colors depict the residual covariance between each pair of populations. Darker colors indicate populations more closely related to each other than expected under a bifurcating maximum likelihood tree, suggestive of gene flow.

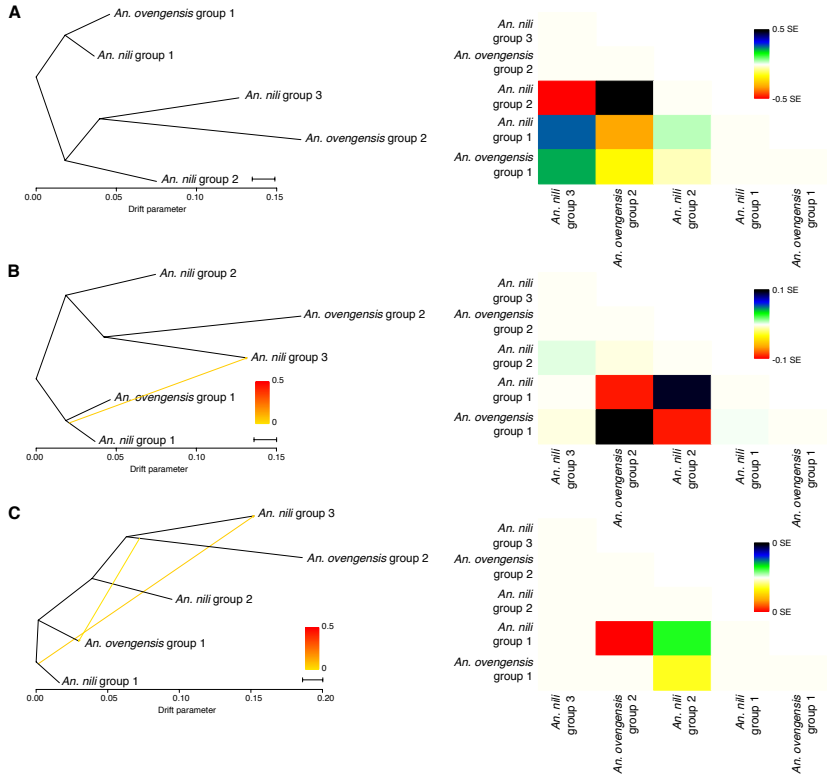

858 **Figure 3**: Frequency distribution of F_{ST} (A) and d_{xy} (B) based on 9622 variant sit

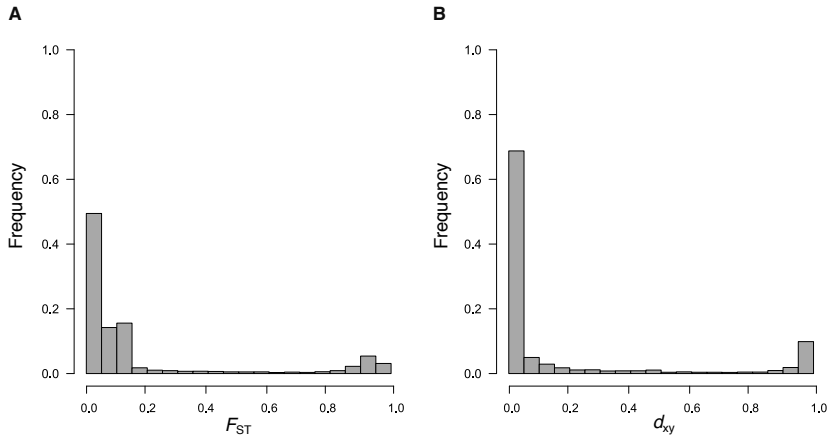

859

Figure 4: Results of Linkage disequilibrium analyses in LDna. (A) LDna graph suggesting the presence of 6 LD clusters (Single Outlier Clusters (SOCs)) based on 1330 SNPs in a dataset containing *An. nili*, *An. ovengensis,* and hydrids of the two species. Values of the two parameters: φ (which controls when clusters are defined as outliers) and $|E|_{\min}$, the minimum number of edges required for a LD cluster to be considered as an outlier, are indicated on top of the graph. Corresponding LD thresholds are shown on the x-axis. (B) Population genetic structure of the six SOCs identified.

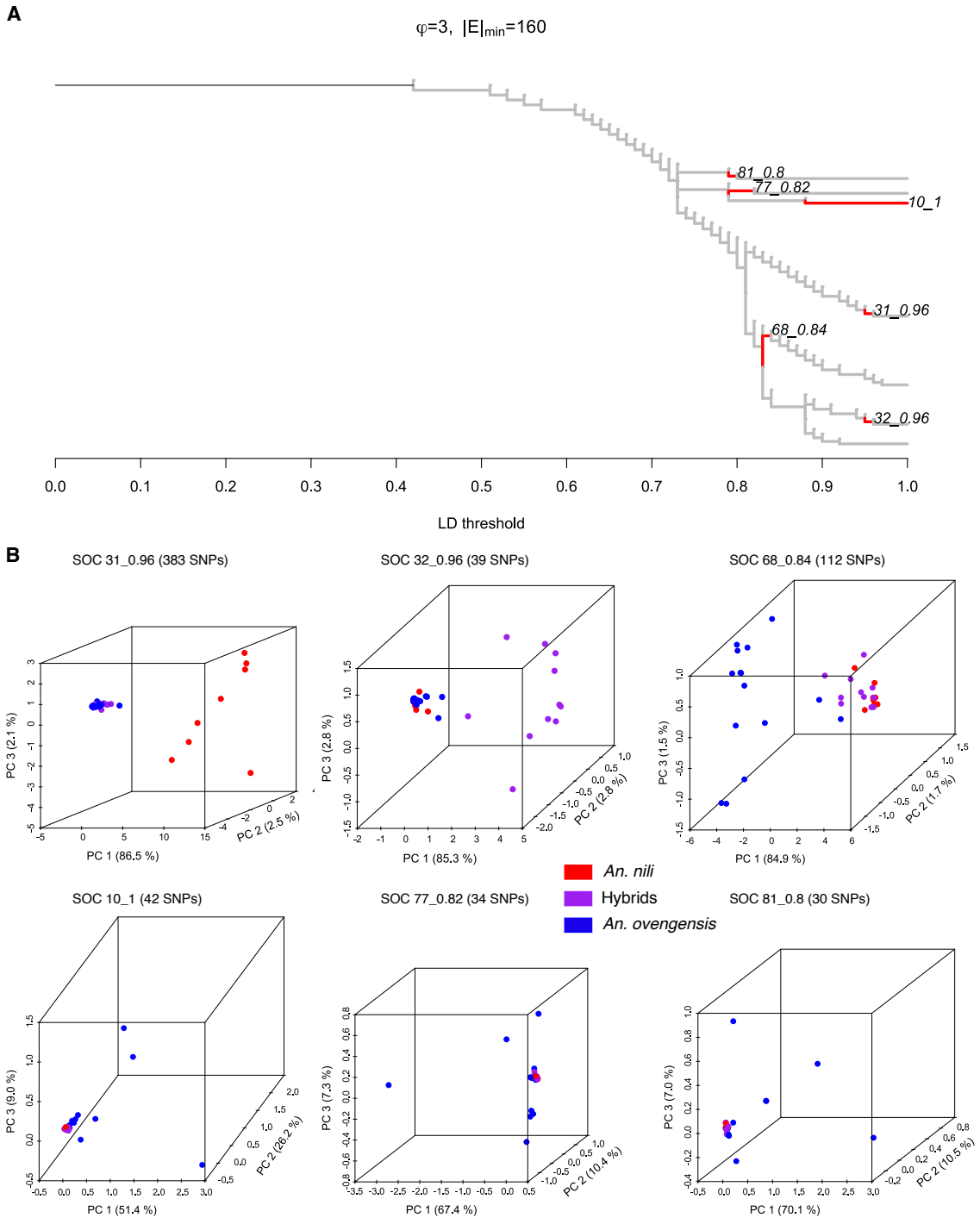

867

868 **Figure 5**: Genomic cline analysis. (A) Frequency distribution of the hybrid index in admixed
869 individuals (hybrid index of pure *An. nili* = 1.0 and pure *An. ovengensis* = 0.0). (B)
870 Prevalence of steep genomic clines illustrated by a scatterplot between the cline
871 parameters α and β.

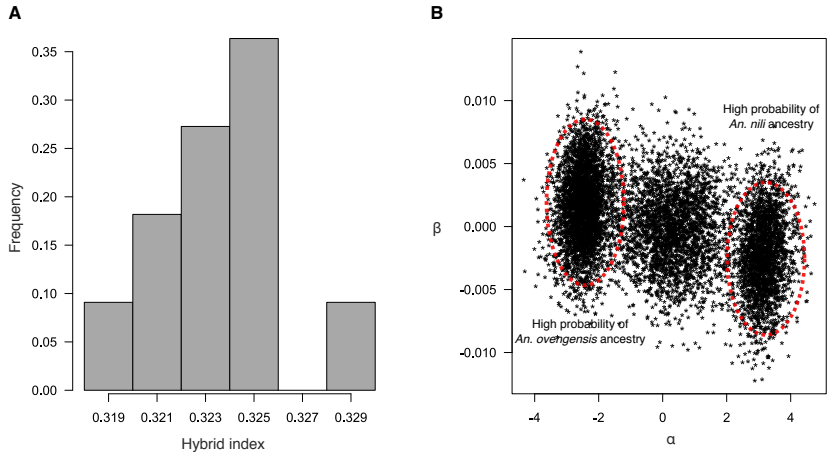

872
873

Supplemental Material

Table S1: Information on *An. nili sensu lato* mosquitoes included in this study.

Sampling locations	Geographic coordinates	Sampling methods			Total
		HLC-OUT	HLC-IN	LC	
Ebebda	4°20'00"N, 11°17'00"E			6	6
Nkoteng	4°31'00"N, 12°02'00"E			8	8
Nyabessan	2°24'00"N, 10°24'00"E	63	44		107
Mbébé	4°10'00"N, 11°04'00"E	13	3	8	24
Total		76	47	22	145

HLC-OUT, human landing catches performed outdoor; HLC-IN, human landing catches performed indoor; LC, larval collection

878 **Table S2**: Pairwise F_{ST} estimated from a *de novo* assembly. p < 0.005 for all values.

F_{ST}	***An. nili* group 1**	***An. nili* group 2**	***An. nili* group 3**	***An. ovengensis* group 1**	***An. ovengensis* group 2**
***An. nili* group 1**	-				
***An. nili* group 2**	0.791	-			
***An. nili* group 3**	0.844	0.862	-		
***An. ovengensis* group 1**	0.705	0.861	0.902	-	
***An. ovengensis* group 2**	0.854	0.862	0.867	0.907	-

879

880 **Table S3**: Results of the most significant f_4 tests for gene flow (*de novo* assembly).

Test	f_4 ± std err	Z-score	P-value
f_4(Oveng 1 ,Nili 3 ; Nili 2, Nili 1)	-0.03692 ± 0.00360	-10.25	<0.00001
f_4(Oveng 1, Nili 3 ; Nili 2, Oveng 2)	0.02787 ± 0.00351	7.94	<0.00001
f_4(Oveng 1, Oveng 2 ; Nili 3, Nili 1)	-0.06610 ± 0.00451	-14.64	<0.00001
f_4(Oveng 1, Oveng 2 ; Nili 2, Nili 1)	-0.04053 ± 0.00368	-11.01	<0.00001
f_4(Nili 3, Nili 1 ; Nili 2, Oveng 2)	-0.02776 ± 0.00349	-7.96	<0.00001

Oveng 1: *An. ovengensis* group 1 ; Oveng 2: *An. ovengensis* group 2 ; Nili 1: *An. nili* group 1 ; Nili 2: *An. nili* group 2 ; Nili 3: *An. nili* group 3

Figure S1: Population genetic structure of *An. nili sensu lato* inferred from 3071 SNPs identified with a *de novo* assembly. (A) ADMIXTURE plots with k from 2 trough 8. (B) and (C) neighbor-joining tree and PCA. (D), (E) and (F) Identification of the optimal number of genetic clusters using the delta k method of Evanno et al, DAPC, and a 10-fold cross-validation in ADMIXTURE.

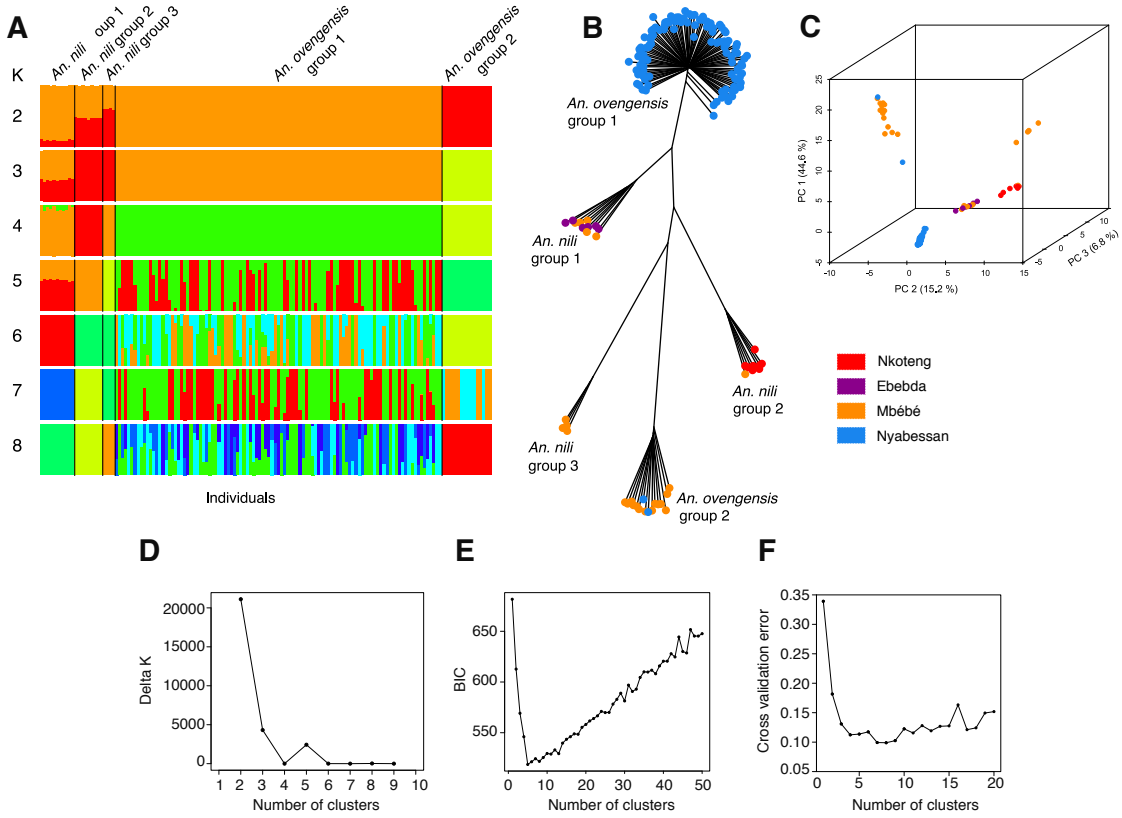

Figure S2: *TreeMix* Maximum Likelihood (ML) trees estimated from 3071 SNPs identified with a *de novo* assembly. ML tree and residual fit from the ML model inferred with (A) no migration, (B) a single migration and (C) two migration edges. See Fig. 2. in the main text for additional description.